

Repression of the Type I Interferon pathway underlies MYC & KRAS-dependent evasion of NK & B cells in Pancreatic Ductal Adenocarcinoma

Nathiya Muthalagu¹, Tiziana Monteverde², Ximena Raffo-Iraolagoitia¹, Robert Wiesheu², Declan Whyte², Ann Hedley¹, Sarah Laing², Björn Kruspig², Rosanna Upstill-Goddard³, Robin Shaw¹, Sarah Neidler², Curtis Rink¹, Saadia A. Karim¹, Katarina Gyuraszova², Colin Nixon¹, William Clark¹, Andrew V. Biankin³, Leo M. Carlin^{1,2}, Seth B. Coffelt^{1,2}, Owen J. Sansom^{1,2}, Jennifer P. Morton^{1*} & Daniel J. Murphy^{1,2*}

Summary of Supplementary Materials:

Supplementary Figures 1-6

Supplementary Tables 1-3

Supplementary Table S4 (provided as a separate Excel file)

Detailed RNA-SEQ Materials & Methods

Supplementary References

Figure S1

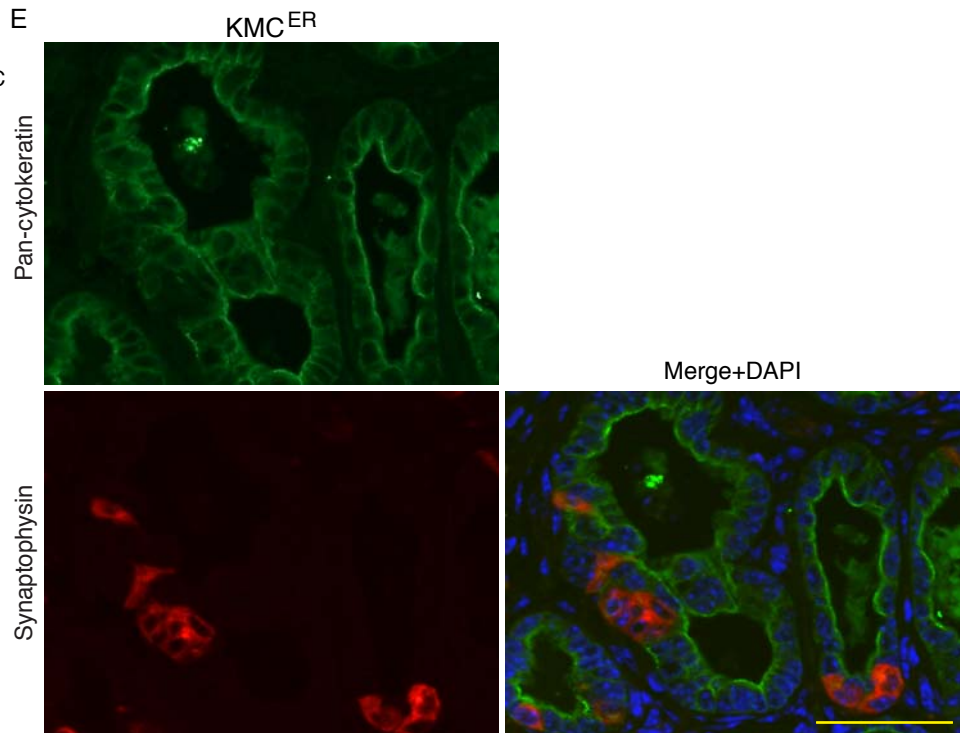
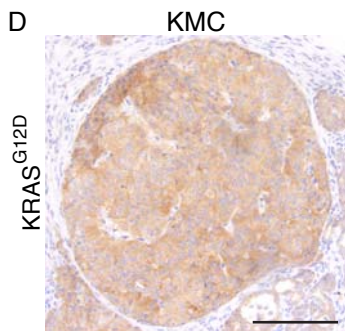
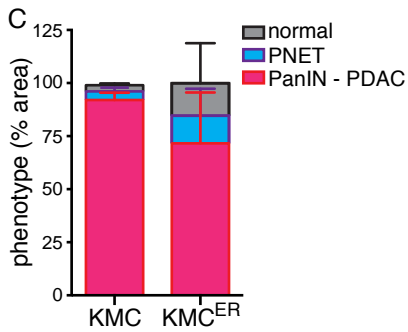
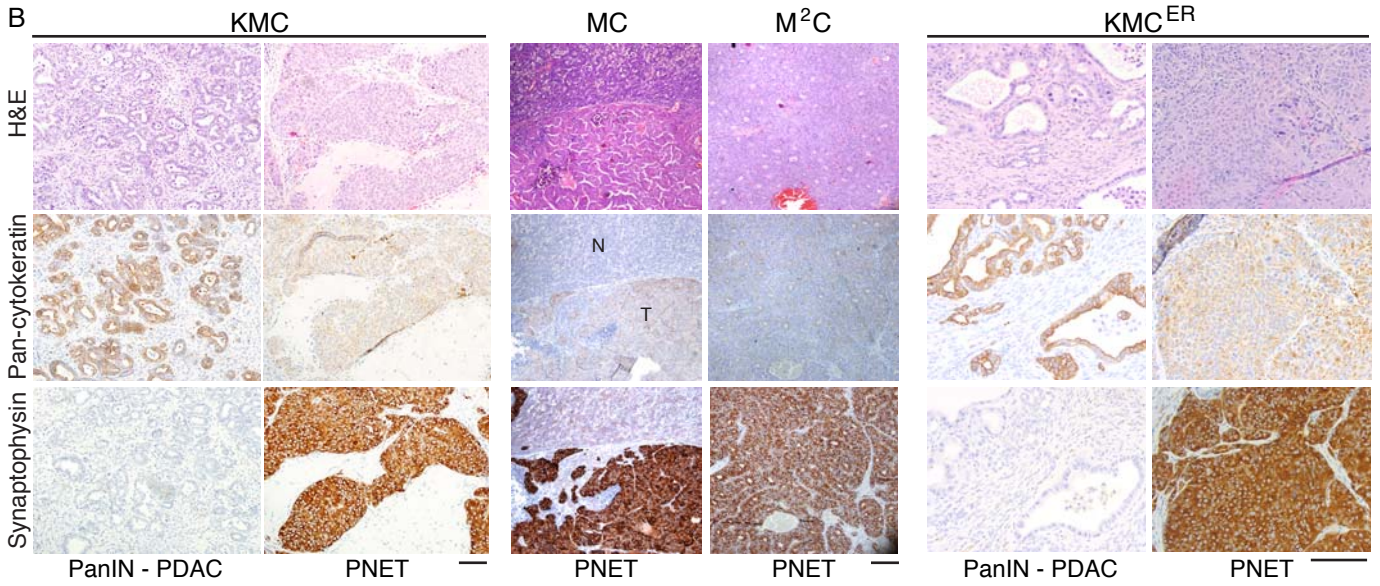
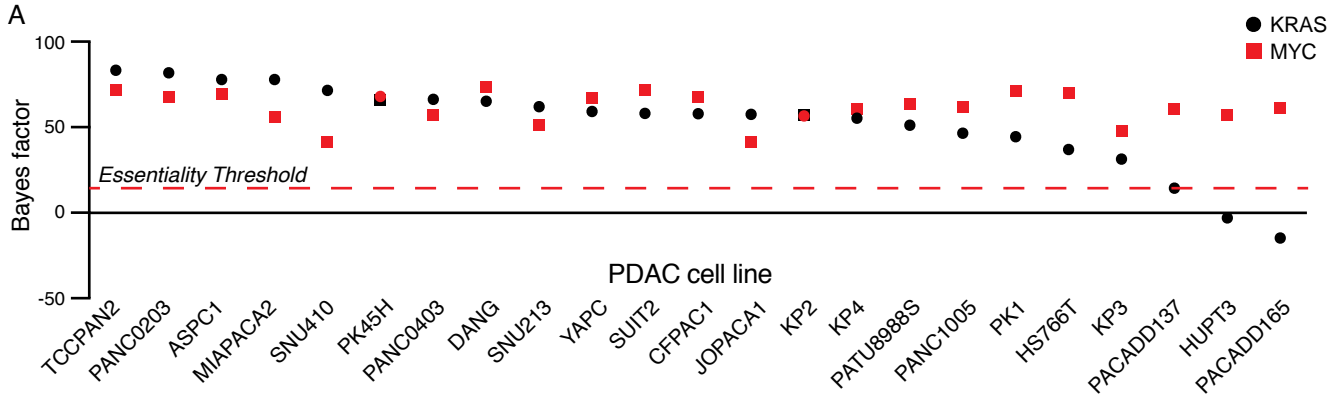


Figure S1: Characterization of MYC-driven pancreatic tumour phenotypes

A) Meta-analysis of CRISPR deletion of *KRAS* or *c-MYC* in human PDAC cell lines using the Avana 2018 gRNA library, generated using the PICKLES database: <https://hartlab.shinyapps.io/pickles/>. A Bayes factor >5 indicates essentiality of each gene for the indicated cell line. **B)** Histological characterization of tumours in mice of the indicated genotypes. For KMC and KMC^{ER}, representative images of both ductal epithelial lesions and neuroendocrine tumour areas are shown. N = normal pancreas; T = tumour. Scale bars = 100µm. **C)** Quantification of tumour area showing features of PanIN-PDAC versus PNET or normal tissue in KMC (N=11) and KMC^{ER} (N=10) mice. **D)** IHC staining with KRas^{G12D}-specific antibody shows expression of mutant KRAS in an area of PNET. Scale bar = 1000 µM. **E)** Immunofluorescent detection of cytokeratin and synaptophysin double-positive cells in KMC^{ER} tumour tissue. Scale bar = 50 µM.

Figure S2

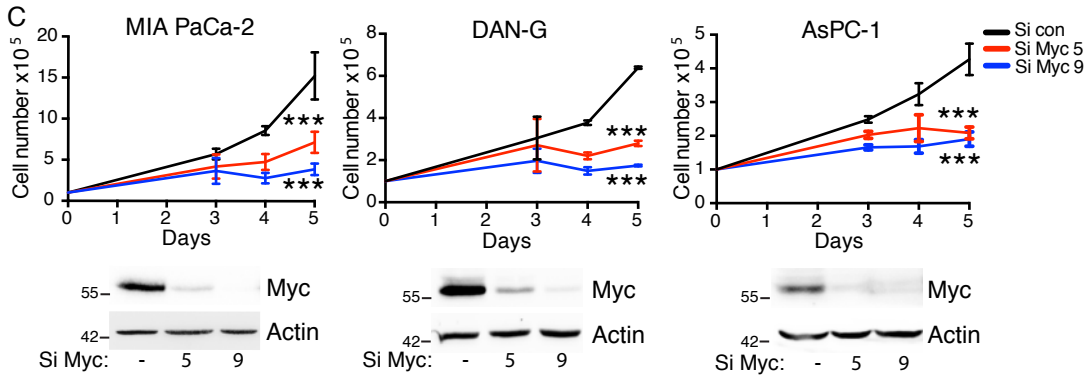
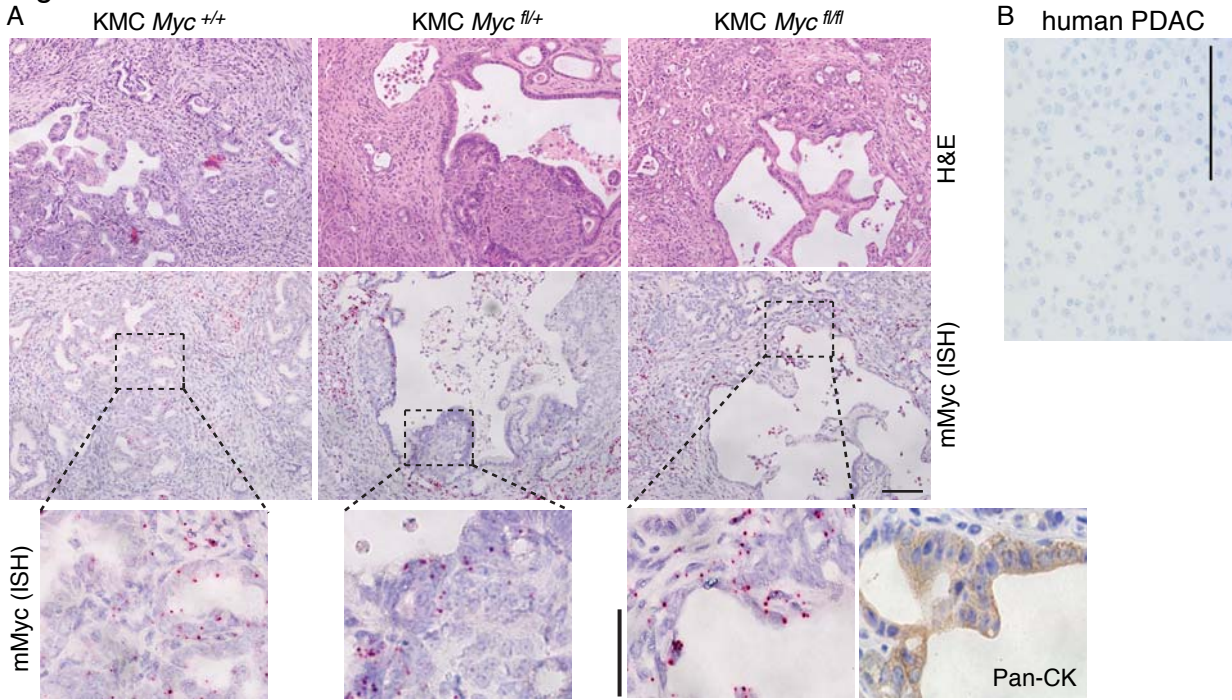


Figure S2: Expression of endogenous c-Myc is required for KMC PDAC development

A) *In situ* hybridization for murine *c-Myc* in PDAC from KMC, KMC-*cMyc*^{fl/+} and KMC-*cMyc*^{fl/fl} mice (red stain). Note the retention of expression in ductal epithelium of KMC-*cMyc*^{fl/fl} tumours. Scale bars = 100µm (main panels) and 50µm (zoomed insets). **B)** ISH staining of a section of human PDAC using the same murine *c-Myc*-specific probe as in (A). Scale bar = 100µm. **C)** Cell propagation measurement upon depletion of MYC in 3 human PDAC cells lines using either of 2 siRNAs. N=3 independent experiments. *** denotes p<0.001 (ANOVA, Dunnett's multiple comparisons test). Lower panels: Immunoblots confirm MYC depletion.

Figure S3

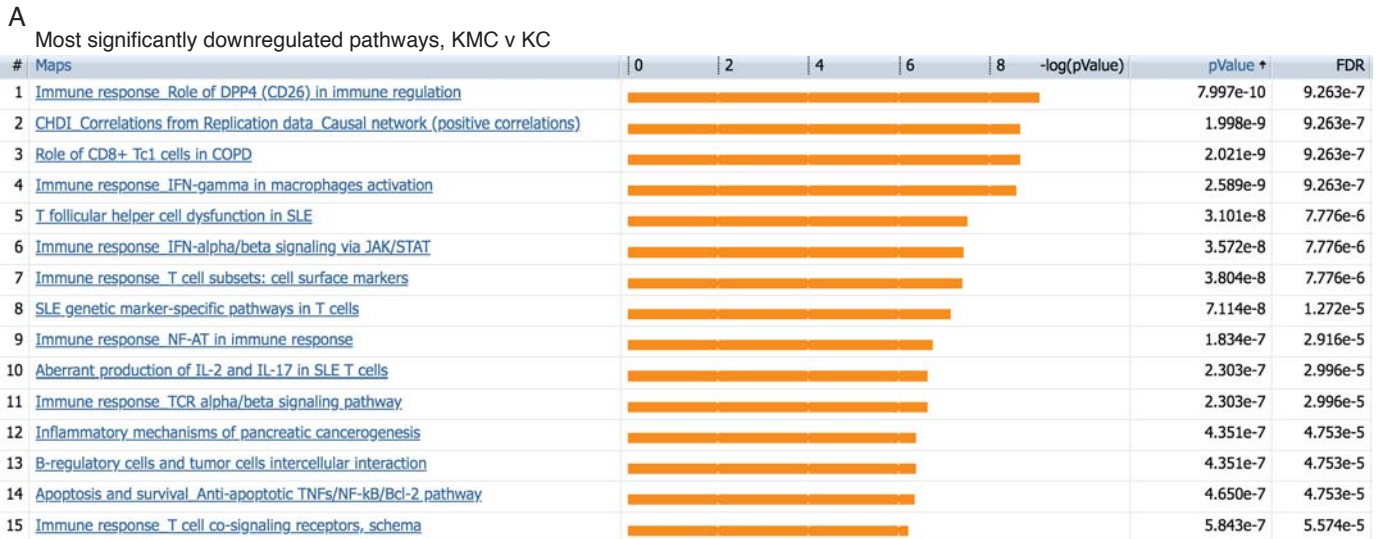


Figure S3: MYC levels modulate the immune landscape in PDAC

Metacore GeneGO analysis of RNA SEQ data from KC (N=6) versus KMC (N=6) tumours, showing the top 15 most significantly downregulated pathways in KMC, relative to KC PDAC tumours. FDR = false discovery rate.

Pathway annotations current as of January 2020.

Figure S4

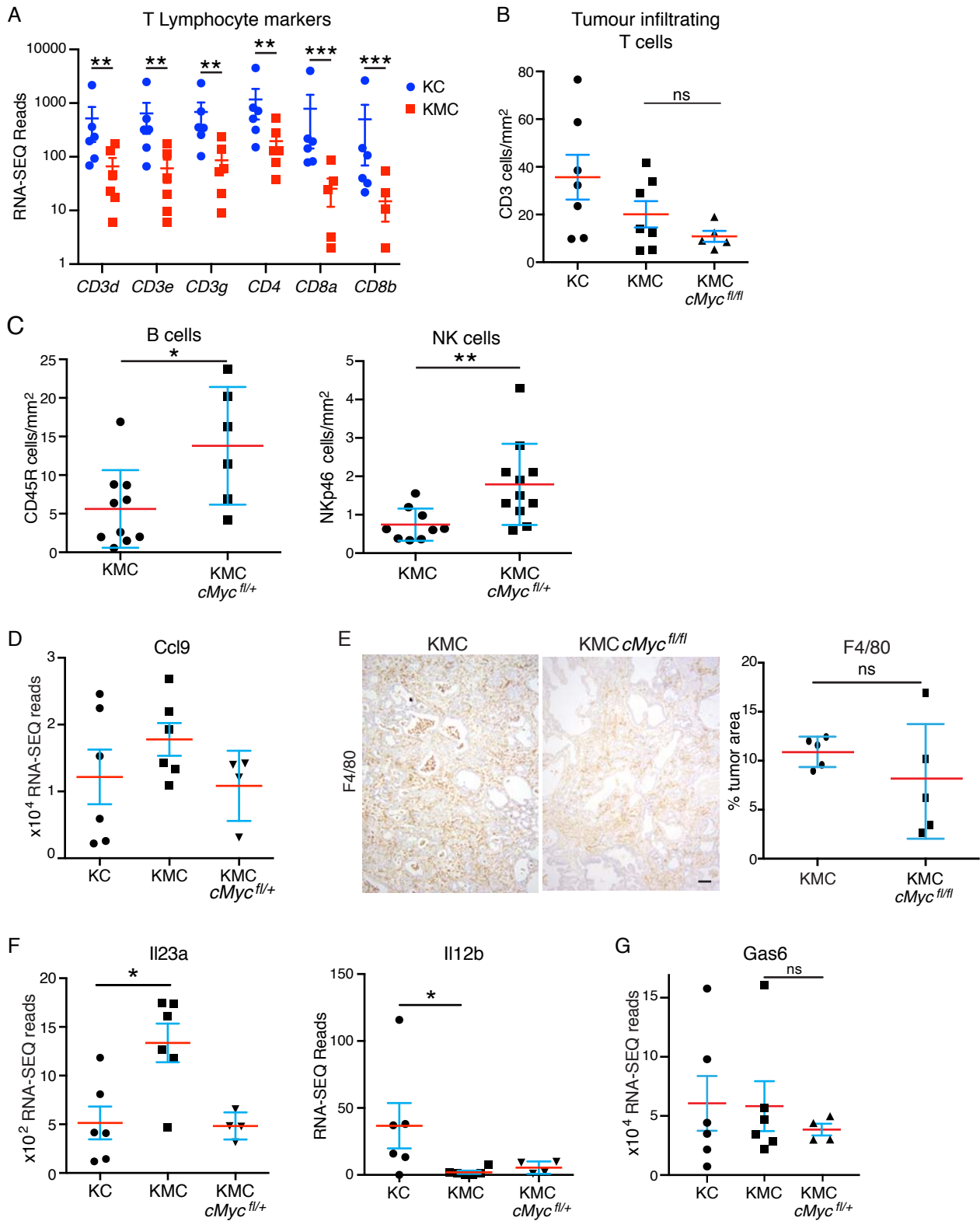


Figure S4: Previously described mechanisms fail to account for long-term effects of MYC on the immune landscape of PDAC

A) RNA-SEQ analysis of T lymphocyte gene expression in KC (N=6) versus KMC tumours (N=6). Mean and SEM values shown (panels A-G). Note that samples with zero reads are omitted from log scale graphics (pertains only to KMC samples). **B)** IHC quantification of CD3-positive T cell tumour infiltration in KC (N=7), KMC (N=7) and KMC-*Myc^{fl/fl}* (N=5) PDAC; ns = not significant, Kruskal-Wallis and Dunn's multiple comparison test. **C)** IHC quantification of CD45R-positive B and NKp46-positive NK cell tumour infiltration in KMC versus KMC-*Myc^{fl/+}* PDAC. * denotes P<0.05, ** denotes P<0.01. Mann-Whitney test. **D)** RNA-SEQ analysis of *Ccl9* expression in KC (N=6), KMC (N=6) and KMC-*Myc^{fl/+}* (N=4) PDAC. **E)** IHC quantification of F4/80 positive macrophage infiltration, measured as % tumour area, in KMC (N=5) versus KMC-*Myc^{fl/fl}* (N=5) PDAC. Scale bar = 100µm; ns = not significant, Mann-Whitney test. **F)** RNA-SEQ analysis of IL23 subunit expression in KC (N=6), KMC (N=6) and KMC-*Myc^{fl/+}* (N=4) PDAC. * denotes P<0.05. ANOVA and post-hoc Tukey test. **G)** RNA-SEQ analysis of Gas6 expression in KC (N=6), KMC (N=6) and KMC-*Myc^{fl/+}* (N=4) PDAC. ANOVA and post-hoc Tukey test; ns = not significant.

Figure S5

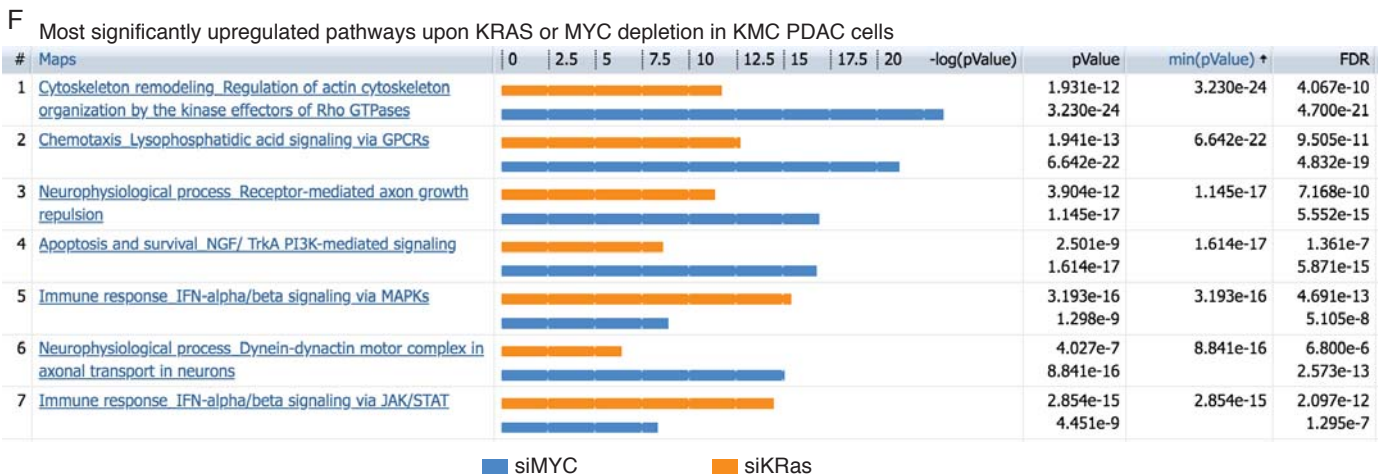
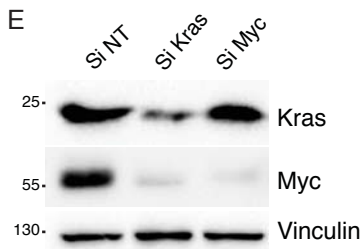
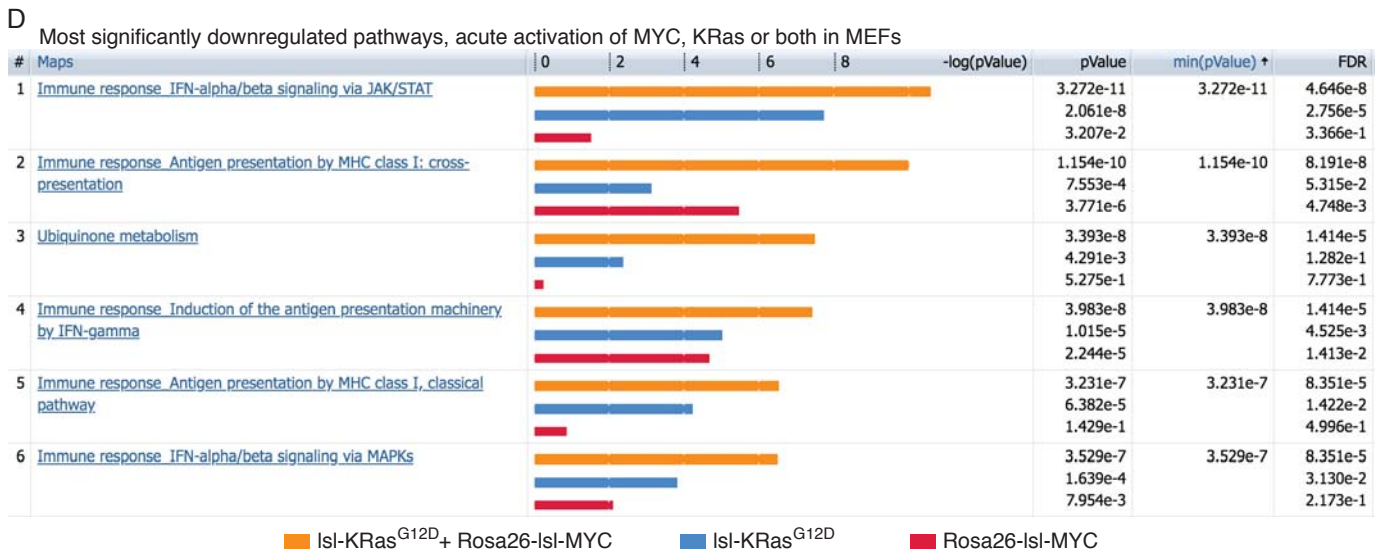
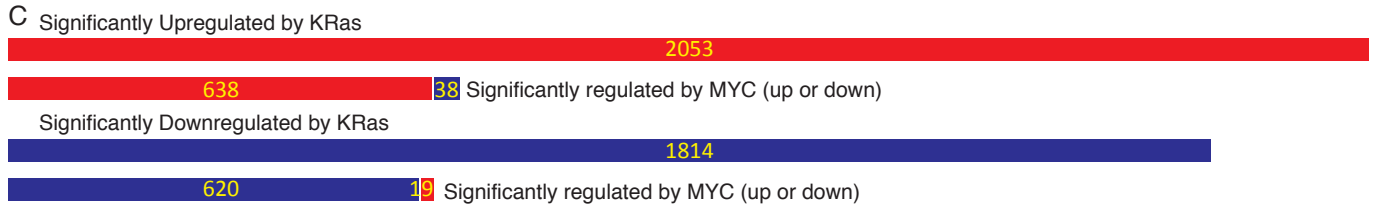
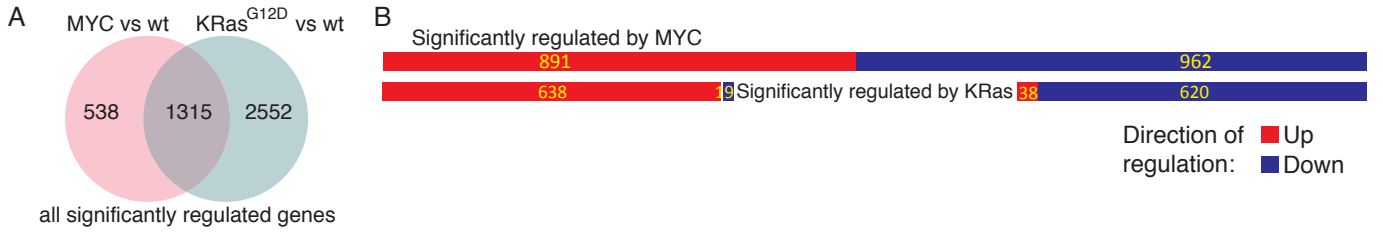


Figure S5: Coordinate regulation of gene expression by KRAS and MYC in PDAC & MEFs

A) Summary of RNA-SEQ analysis showing overlap in significantly altered gene expression (irrespective of direction or magnitude change), relative to control infected MEFs, upon acute CRE-mediated activation of *Isl-KRas^{G12D}* and *Rosa26^{DM-Isl-MYC}* alleles. Numbers indicate the number of significantly regulated genes. **B)** Co-directional gene regulation of MYC-regulated genes upon activation of KRas^{G12D}, as per (A). Numbers indicate the number of significantly regulated genes. **C)** Co-directional regulation of KRas^{G12D}-regulated genes upon expression of Rosa26-driven MYC, as per (B). **D)** Metacore GeneGO analysis of the most significantly down-regulated pathways upon activation of *Isl-KRas^{G12D}*, *Rosa26^{DM-Isl-MYC}* or both in MEFs. Coloured bars indicate p values (-log). **E)** Immunoblots showing depletion of MYC and KRAS in KMC PDAC tumour cells treated with the indicated siRNAs. **F)** Metacore GeneGO analysis of RNA-SEQ data from KMC PDAC tumour cells upon siRNA-mediated depletion of MYC (N=4) or KRas (N=4) *in vitro*. MYC was depleted using pooled siRNA targeting both human and murine *c-MYC*.

Figure S6

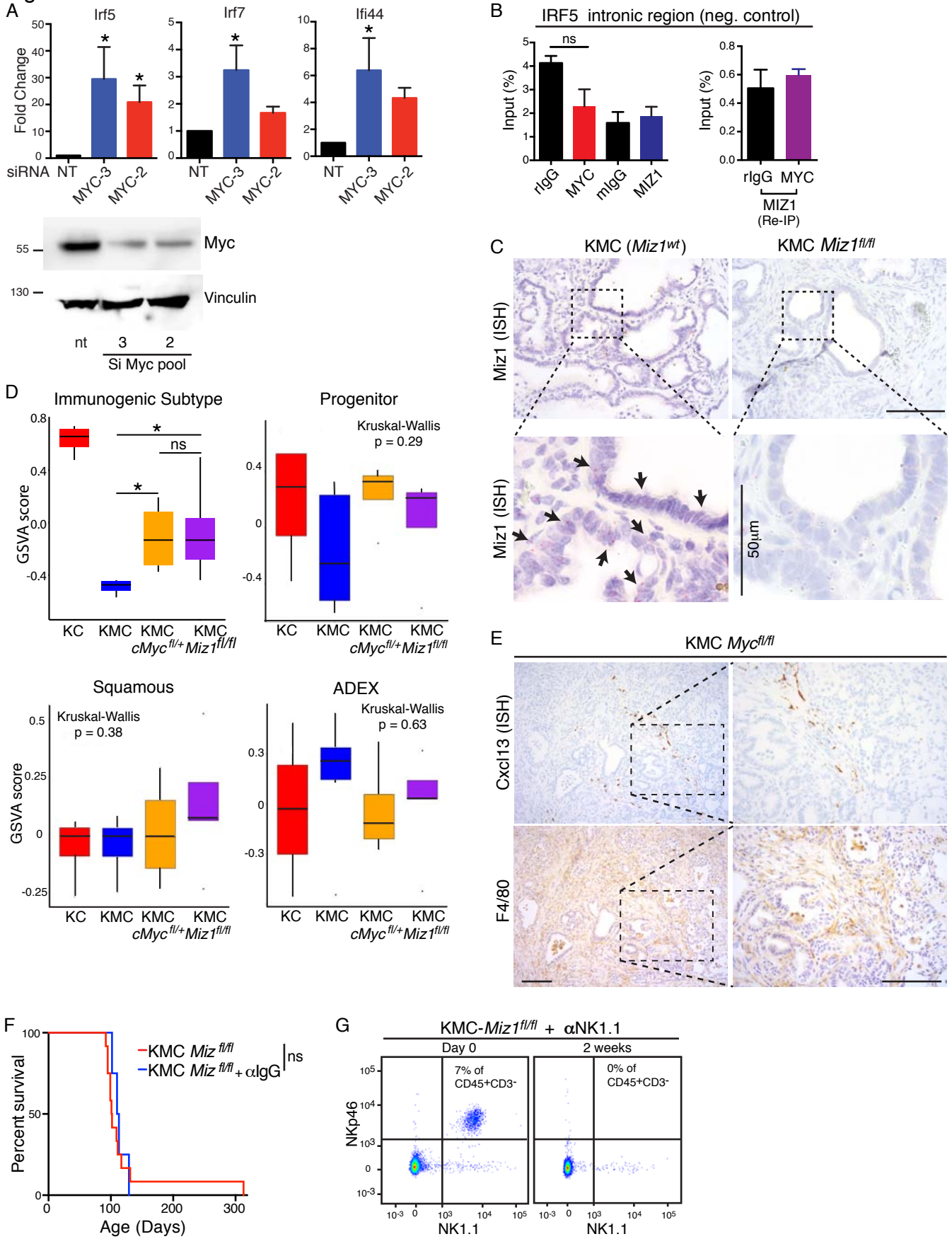


Figure S6: The role of Miz1 in MYC-dependent suppression of the immune landscape

A) Q-PCR analysis of expression of indicated genes in KMC PDAC cells upon depletion of MYC (human & murine) with either of 2 pools of siRNA. Mean and SEM of 3 independent experiment shown. * denotes $P < 0.05$, ANOVA and Fisher's LSD test. Immunoblot (right panel) confirms MYC depletion. **B)** Chromatin immunoprecipitation (ChIP) and ChIP-re-ChIP analysis of MYC and MIZ1 binding to an intronic region of the human IRF5 locus in DAN-G cells. Mean and SEM of technical replicates from 1 of 3 independent experiments shown; ns= not significant, ANOVA and Tukey's multiple comparison test. **C)** ISH analysis showing effective deletion of *Miz1* in KMC-*Miz1*^{fl/fl} PDAC ductal epithelium. **D)** PDAC subtype analysis performed as per Bailey et al. (1) showing the impact of *c-Myc* or *Miz1* deletion in KMC tumours upon the murine equivalent of the human "immunogenic" subtype but none of the other three subtype gene signatures. Data derived from RNA-SEQ analysis of tumours from the indicated genotypes. * denotes $P < 0.05$, Kruskal-Wallis and Dunn's multiple comparison test. **E)** Expression of *Cxcl13* detected in KMC-*Myc*^{fl/fl} PDAC tumours by ISH. Lower panels show F4/80 IHC. Scale bars = 50 μ m. **F)** Survival analysis upon treatment of KMC-*Miz1*^{fl/fl} tumour-bearing mice with Goat IgG isotype control for anti-Cxcl13 (N=4) versus no treatment (N=12). **G)** Representative FACS analysis of whole blood from KMC *Miz1*^{fl/fl} mouse before or after 2 weeks treatment with NK1.1 depleting antibody. N = 3.

Table S2: Significantly regulated by KRas^{G12D} in MEFs

Table shows RNA-SEQ reads for each gene significantly regulated by more than 2 fold upon activation of Isl-KRas^{G12D} allele for 24hrs in primary MEFs. Comparison is with identically treated passage-matched wild-type MEFs. FC = fold change, numbers >2 in red, <-2 in dark blue. Adjusted p values <0.05 shown in red. Also shown are RNA-SEQ reads for the same genes upon similar activation of Rosa26^{DM-Isl-MYC}, compared with wt MEFs, using the same colour scheme, plus FC>1.5 in pink; <-1.5 in light blue, to highlight convergent and divergent gene expression.

Muthalagu et al. Table S3: Significantly regulated by KRasG12D+Rosa26-DM-MYC in MEFs

gene_name	symbol	Mean WT	Mean MycKras	FC	padj
aggrecan	Acan	43.2824021	660.527155	8.72130989	4.3253E-84
glucosaminyl (N-acetyl) transferase 1, core 2	Gcnt1	27.7489748	196.0805209	4.54473728	1.1057E-31
gap junction protein, beta 2	Gjb2	466.955423	2364.985825	4.4734454	2.0759E-69
chemokine (C-X-C motif) ligand 3	Cxcl3	8.98697059	94.71136401	4.04589344	2.8361E-22
elastin	Eln	45.1426709	439.011641	4.02905949	2.2919E-19
early growth response 1	Egr1	119.989019	767.9263895	4.00565515	6.2083E-25
CAP-GLY domain containing linker protein family, member 4	Clip4	47.8791174	254.6629093	3.83665229	2.5113E-31
BarH-like homeobox 1	Barx1	1.82270046	54.87072145	3.61275007	2.339E-16
integrin alpha 2	Itga2	403.501296	1888.796944	3.50096975	2.8319E-24
paired-like homeodomain transcription factor 1	Pitx1	57.4823739	245.0427559	3.22606801	1.9355E-21
solute carrier family 4 (anion exchanger), member 4	Slc4a4	416.774414	1391.747637	3.13830216	1.9212E-58
pro-platelet basic protein	Ppbb	281.783911	952.7617401	3.05332845	2.8675E-33
nuclear receptor subfamily 1, group H, member 5	Nr1h5	14.0005099	88.86336074	3.02592418	1.2637E-12
ATPase, H ⁺ transporting, lysosomal V0 subunit E2	Atp6v0e2	39.8441402	154.8247926	2.95212193	6.3004E-17
chemokine (C-X-C motif) ligand 12	Cxcl12	1184.25058	3660.38941	2.84973329	1.4587E-37
angiopoietin-like 7	Angptl7	16.4852509	89.58234157	2.61277018	1.5142E-11
plakophilin 1	Pkp1	247.243603	735.1157984	2.79493142	8.5981E-34
S100 calcium binding protein A16	S100a16	194.164971	610.8912967	2.76495743	3.9614E-26
complement component 1, s subcomponent 1	C1s1	20.503079	92.90708547	2.67849947	3.9917E-11
matrix metalloproteinase 3	Mmp3	136.749548	388.1413648	2.61628812	4.5829E-22
insulin-like growth factor 2	Igf2	912.105521	2743.793326	2.6156507	3.0533E-18
solute carrier family 14 (urea transporter), member 1	Slc14a1	43.1917414	142.279444	2.55847704	4.7713E-11
solute carrier family 29 (nucleoside transporters), member 2	Slc29a2	231.60392	693.2518481	2.5161548	7.7344E-15
protein tyrosine phosphatase, non-receptor type 13	Ptpn13	2319.43332	6292.845664	2.47729156	6.2862E-23
chemokine (C-X-C motif) ligand 5	Cxcl5	326.105364	1015.029521	2.46134975	1.2897E-11
5' nucleotidase, ecto	Nt5e	364.391148	948.3364829	2.4534367	2.5556E-43
neuronal cell adhesion molecule	Nrcam	154.069126	405.2908065	2.45275411	1.0552E-22
solute carrier family 17 (sodium-dependent inorganic phosphate cotransporter), member 6	Slc17a6	21.3287104	72.05974685	2.44233379	8.5243E-09
TraB domain containing 2B	Trabd2b	108.71626	323.800266	2.4268601	6.4063E-12
peptidase inhibitor 15	Pi15	300.065366	772.8549345	2.40254069	3.5911E-25
leucine rich repeat transmembrane neuronal 2	Lrrtm2	157.096374	452.4045032	2.39798828	2.4869E-12
angiotensin II receptor, type 2	Agtr2	15.7793228	63.09436434	2.37747528	6.8206E-09
unc-13 homolog C (C. elegans)	Unc13c	166.588113	446.5198225	2.3726152	3.0654E-20
E2F transcription factor 8	E2f8	446.019925	1282.780131	2.35597781	4.5548E-11
aristaless-like homeobox 3	Alx3	11.6796992	51.00408659	2.35214561	1.1618E-07
collagen, type XIV, alpha 1	Col14a1	356.822992	997.6342172	2.3360876	1.1259E-11
neuronal guanine nucleotide exchange factor	Ngef	110.62466	290.5733401	2.31492917	7.6643E-14
HtraA serine peptidase 3	Htra3	128.55064	395.6963846	2.31208268	1.2681E-08
alanyl (membrane) aminopeptidase	Anpep	16.1140118	78.06614769	2.30063755	4.7562E-07
dynactin associated protein	Dynap	135.395406	355.4514782	2.3001447	1.8935E-15
anoctamin 1, calcium activated chloride channel	Ano1	510.991344	1282.927235	2.29657399	3.222E-21
inositol polyphosphate-4-phosphatase, type II	Inpp4b	38.647779	128.9562996	2.29337157	9.4866E-09
interleukin 11	Il11	361.891052	865.667004	2.28880643	9.2992E-26
mesothelin	Msln	94.8803598	235.8996116	2.27843511	1.9754E-14
transcription factor AP4	Tfap4	219.96692	541.1771647	2.27088676	1.5009E-19
BTB (POZ) domain containing 11	Btbd11	395.548323	974.1622865	2.26804115	1.6953E-22
secreted phosphoprotein 1	Spp1	8558.83351	20824.18223	2.2642879	5.0037E-20
uncoupling protein 2 (mitochondrial, proton carrier)	Ucp2	367.949283	932.1181487	2.23283864	2.3911E-13
lumican	Lum	63.0348167	170.3432406	2.21496348	3.8988E-09
RIKEN cDNA 1700012B09 gene	1700012B09	35.7824245	99.24117258	2.20652483	4.9675E-08
collagen, type XV, alpha 1	Col15a1	181.236837	488.6881144	2.20494558	3.3312E-09
aquaporin 1	Aqp1	1619.79319	3686.133335	2.20375796	5.4711E-42
high mobility group AT-hook I, related sequence 1	Hmga1-rs1	5094.28082	11675.17447	2.20318228	7.5195E-31
tropomodulin 2	Tmod2	264.580741	637.6939635	2.20010036	2.8043E-17
expressed sequence AI854703	AI854703	7.08230498	30.85897026	2.18256861	4.8729E-06
potassium voltage-gated channel, subfamily Q, member 5	Kcnq5	215.999978	517.1273532	2.18213624	4.8225E-22
ribosomal protein L35A	Rpl35a	262.829783	628.5910554	2.16756141	1.1815E-13
fibroblast growth factor 10	Fgf10	436.392758	1040.427576	2.15730709	4.9993E-15
protein tyrosine phosphatase, non-receptor type 22 (lymphoid)	Ptpn22	18.5545258	58.72308617	2.15492829	1.1384E-06
SRY (sex determining region Y)-box 2	Sox2	1.7407353	31.27556278	2.13456412	1.0552E-05
treacle ribosome biogenesis factor 1	Tcof1	1426.34483	3515.810541	2.13369332	6.505E-10
neuronal pentraxin 1	Nptx1	62.2079972	154.9921632	2.1292723	1.7548E-09
heparan sulfate (glucosamine) 3-O-sulfotransferase 1	Hs3st1	33.797491	96.35717858	2.11674296	2.4426E-07
solute carrier organic anion transporter family, member 2a1	Slco2a1	706.396386	1682.816281	2.10184339	1.296E-10
family with sequence similarity 84, member A	Fam84a	57.7738543	138.6790084	2.07393404	9.1553E-08
paired-like homeodomain transcription factor 2	Pitx2	35.3300689	93.12904054	2.07171447	1.786E-07
suprabasin	Sbsn	275.542252	605.1940891	2.06599509	1.5494E-16
cDNA sequence BC048403	BC048403	95.9687685	286.4009379	2.05846599	8.9413E-06
immunoglobulin superfamily, DCC subclass, member 4	Igdcc4	164.432421	392.1430876	2.05313107	3.1167E-09
delta-like 1 homolog (Drosophila)	Dlk1	903.19726	2256.644499	2.04900392	3.7725E-07
autism susceptibility candidate 2	Auts2	184.062926	442.3620265	2.04896119	1.0349E-08
mitogen-activated protein kinase 6	Mapk6	9710.89006	21504.09072	2.03999985	1.6452E-12
histone cluster 2, H4	Hist2h4	548.593784	1238.962513	2.03180415	4.0673E-10
histone H4	LOC1026412	548.593784	1238.962513	2.03180415	4.0673E-10
RIKEN cDNA D630045J12 gene	D630045J12	125.532936	295.9722922	2.02439498	8.5567E-08
teneurin transmembrane protein 4	Tenm4	518.878455	1169.028293	2.01159066	7.2554E-10
dual specificity phosphatase 5	Dusp5	1871.02166	3908.14032	2.00997903	9.0078E-22
forkhead box G1	Foxg1	178.634599	395.5432177	2.00713522	5.4451E-11
elastin microfibril interfacier 2	Emilin2	1490.22016	3202.722406	2.00332407	4.0013E-13

proline arginine-rich end leucine-rich repeat family with sequence similarity 131, member A	Prelp	41.7037301	131.8208943	2.00052337	4.6195E-05
integrin alpha 1	Fam131a	137.008591	62.19531699	-2.0037806	1.905E-09
colony stimulating factor 3 (granulocyte)	Itga1	1202.2431	573.1027717	-2.0046094	1.3395E-17
sodium channel, voltage-gated, type IX, alpha	Csf3	97.5283522	34.20659012	-2.0107963	1.7073E-05
apolipoprotein E	Scn9a	26.2155482	3.238997904	-2.0137925	1.6612E-05
signal transducer and activator of transcription 2	Apoe	227.811032	92.7521333	-2.0183322	3.2224E-07
relaxin family peptide receptor 3	Stat2	516.539366	219.0429329	-2.0206629	6.1262E-08
leucine rich adaptor protein 1-like	Rxfp3	66.2254858	25.48563631	-2.0218288	4.0325E-06
complement receptor 2	Lurap1l	7727.90395	3572.800699	-2.0245457	2.4103E-14
histocompatibility 2, M region locus 9	Cr2	51.2716247	16.32053798	-2.025147	3.9435E-05
2'-5' oligoadenylate synthetase-like 2	H2-M9	58.8530583	21.06952806	-2.0274305	1.2697E-05
solute carrier family 5 (choline transporter), member 7	Oasl2	148.893523	59.46124755	-2.0302615	7.2023E-07
collagen, type XIX, alpha 1	Slc5a7	1077.10637	504.8016549	-2.0304789	3.6236E-20
Fc receptor-like 5, scavenger receptor	Col19a1	154.72298	63.32499166	-2.039001	3.6006E-08
regulator of G-protein signaling 17	Fcrls	28.9465242	2.456358016	-2.0406097	1.0841E-05
poly (ADP-ribose) polymerase family, member 10	Rgs17	556.418868	257.8992665	-2.0423032	5.1789E-22
predicted gene 11627	Parp10	250.856358	110.1328546	-2.0490297	2.2967E-11
H6 homeobox 1	Gm11627	59.9310741	22.46576914	-2.0511706	4.3037E-06
growth arrest specific 6	Hmx1	27.3318114	4.585264129	-2.0546842	3.0596E-05
ubiquitin-like modifier activating enzyme 7	Gas6	12192.2078	5621.318529	-2.0577779	1.5017E-18
3-hydroxyacyl-CoA dehydratase 4	Uba7	154.134888	55.44497327	-2.0589803	2.7643E-06
solute carrier family 9 (sodium/hydrogen exchanger), member 2	Hacd4	1220.58051	576.6124299	-2.0594458	9.2351E-36
calponin 1	Slc9a2	121.430937	48.14517182	-2.059999	2.4887E-07
potassium inwardly-rectifying channel, subfamily J, member 15	Cnn1	23237.2368	10540.96748	-2.0650551	1.2391E-15
hydroxyprostaglandin dehydrogenase 15 (NAD)	Kcnj15	543.67994	250.4940698	-2.0674358	1.1015E-19
gap junction protein, alpha 5	Hpgd	17.2290868	1.801337024	-2.0685058	1.6288E-05
membrane bound O-acyltransferase domain containing 2	Gja5	31.103744	6.109006919	-2.0738783	2.5653E-05
interferon induced transmembrane protein 1	Mboat2	1141.56361	531.7237451	-2.074678	2.1215E-24
vanin 1	Ifitm1	56.5303805	17.98304468	-2.0757661	1.1737E-05
SLAM family member 9	Vnn1	90.6256712	36.87086744	-2.075802	2.5404E-07
sialic acid binding Ig-like lectin G	Slamf9	96.3751996	35.03607974	-2.0764284	2.3923E-06
leucine zipper, putative tumor suppressor 1	Siglecg	3279.74261	1524.628809	-2.0765181	1.3713E-28
urotensin 2B	Lzts1	33.0082399	8.104747016	-2.0817596	2.7369E-05
colony stimulating factor 1 receptor	Uts2b	30.9775517	5.398581139	-2.0846884	2.4183E-05
coiled-coil domain containing 109B	Csf1r	155.474493	65.83160968	-2.0869723	5.703E-11
discs, large homolog 2 (Drosophila)	Cdccl109b	1763.40645	792.9085818	-2.0929763	2.2324E-17
proteasome (prosome, macropain) subunit, beta type 9 (large multifunctional peptidase 2)	Dlg2	35.3287111	9.350895571	-2.1043066	1.866E-05
proteasome (prosome, macropain) subunit, beta type 8 (large multifunctional peptidase 7)	Psmb9	33.171661	7.333201368	-2.105112	2.0232E-05
neuronatin	Psmb8	209.201646	91.25572378	-2.1095918	1.3462E-12
growth arrest and DNA-damage-inducible 45 beta	Nnat	410.077514	188.4459194	-2.1108308	8.412E-24
hematopoietic cell specific Lyn substrate 1	Gadd45b	1999.75717	885.6799464	-2.1109689	9.5866E-17
solute carrier family 16 (monocarboxylic acid transporters), member 4	Hcls1	26.1716606	3.602674048	-2.1130477	1.2698E-05
late cornified envelope 1G	Slc16a4	231.979611	93.74835681	-2.114531	9.7551E-09
serine (or cysteine) peptidase inhibitor, clade B, member 9	Lce1g	126.35704	48.53386077	-2.1158553	3.6006E-08
phospholipid phosphatase 1	Serpib9	977.128334	425.5520959	-2.1198575	5.5114E-15
integrin alpha M	Plpp1	16317.5589	7372.631142	-2.1305622	7.8599E-28
5-hydroxytryptamine (serotonin) receptor 7	Itgam	29.9068736	5.415222501	-2.1308098	1.2918E-05
Fas (TNF receptor superfamily member 6)	Htr7	169.018404	67.09710674	-2.1314889	6.3519E-09
myosin IF	Fas	347.992993	149.2047095	-2.1349609	1.0588E-12
RIKEN cDNA E030030106 gene	Myo1f	21.7004586	2.539666365	-2.1361889	5.2877E-06
tubulin polymerization-promoting protein family member 3	E030030106R	16.693578	0.979816521	-2.1382339	6.5647E-06
DEAD (Asp-Glu-Ala-Asp) box polypeptide 58	Tppp3	961.243135	426.380101	-2.140408	2.7853E-21
sulfotransferase family 4A, member 1	Ddx58	1695.45791	756.1395665	-2.1454868	6.6648E-27
microtubule associated tumor suppressor candidate 2	Sult4a1	312.441789	134.6661757	-2.147663	8.6022E-17
podocan-like 1	Mtus2	104.617655	40.77638292	-2.1646201	4.5105E-09
interferon, alpha-inducible protein 27 like 2B	Podn1	590.055731	252.3144858	-2.1672797	1.2074E-16
vomeroneasal 2, receptor 79	Ifi2712b	1080.6444	455.7242859	-2.1725355	7.5655E-15
nucleoporin 62 C-terminal like	Vmn2r79	39.5989236	6.977845905	-2.183698	3.7274E-06
CD40 antigen	Nup62cl	1177.71357	487.4879327	-2.1854531	1.1448E-13
R-spondin 3	Cd40	404.591682	172.2584967	-2.1871379	1.694E-19
serine (or cysteine) peptidase inhibitor, clade B, member 9e	Rspo3	326.862857	138.0132603	-2.1873311	1.57E-16
cannabinoid receptor 1 (brain)	Serpib9e	35.2836353	5.900970421	-2.1936269	4.9005E-06
GLI pathogenesis-related 1 (glioma)	Cnr1	233.5057	95.69689561	-2.1955099	8.7026E-14
G protein-coupled receptor 1	Glipr1	2326.70834	981.1081857	-2.2002966	4.948E-18
heat shock protein 1B	Gpr1	242.399464	92.85191506	-2.2162355	1.1631E-10
mannosidase, beta A, lysosomal	Hspa1b	777.396344	336.4784954	-2.2243304	1.4712E-33
Rho guanine nucleotide exchange factor (GEF) 28	Manba	652.632213	278.899354	-2.2280622	1.1002E-29
leucine rich repeat containing 17	Arhgef28	5442.99473	2368.910884	-2.2282216	7.842E-40
TNNI3 interacting kinase	Lrrc17	5204.48312	2188.569634	-2.2405089	5.2665E-23
stabilin 1	Tnni3k	129.220697	46.11655133	-2.2423737	1.0581E-08
X-prolyl aminopeptidase (aminopeptidase P) 2, membrane-bound	Stab1	68.7845148	16.2593517	-2.2650219	1.4641E-06
testis development related protein	Xpnpep2	74.384279	23.16220994	-2.2693074	3.8133E-07
radical S-adenosyl methionine domain containing 2	Tdrp	268.371493	103.215777	-2.2741044	2.4131E-13
fibronectin type III domain containing 5	Rsad2	578.391987	221.7490324	-2.2923461	1.7109E-13
LIM and senescent cell antigen like domains 2	Fndc5	79.8001367	20.47851769	-2.2938709	7.686E-07
receptor transporter protein 4	Lims2	1166.22946	471.6642876	-2.2998673	5.9004E-23
schlafen 2	Rtp4	170.584947	58.25397961	-2.3013025	9.1413E-10
coronin, actin binding protein 1A	Slfn2	222.116803	80.63089328	-2.303594	5.1297E-11
interferon regulatory factor 9	Coro1a	109.467774	36.53237207	-2.3170559	1.1157E-08
membrane-spanning 4-domains, subfamily A, member 6D	Irf9	1013.01507	396.1726594	-2.3173809	1.0639E-17
	Ms4a6d	39.2208561	8.035306467	-2.3186152	1.0627E-06

leukocyte immunoglobulin-like receptor, subfamily B, member 4A	Lilrb4a	25.9261046	1.595956898	-2.3240116	3.2346E-07
fatty acid binding protein 7, brain	Fabp7	140.567065	49.29708574	-2.3340211	6.0849E-11
interferon induced protein with tetratricopeptide repeats 1B like 2	Ifit1bl2	61.2915354	15.08524929	-2.34252	3.0195E-07
CD36 antigen	Cd36	21.536698	2.00949071	-2.3493454	3.5012E-07
basal cell adhesion molecule	Bcam	129.67509	46.92958319	-2.3529653	8.0525E-13
myosin VIIA	Myo7a	424.88928	153.7035558	-2.3544743	1.1509E-12
adhesion G protein-coupled receptor A1	Adgra1	96.8297617	28.12744001	-2.3650885	2.7182E-08
collagen, type VIII, alpha 2	Col8a2	685.604242	275.204883	-2.3775632	1.069E-37
immunity-related GTPase family M member 1	Irgm1	3314.20491	1323.852711	-2.3924187	5.2874E-38
popeye domain containing 2	Popdc2	218.848451	81.62469479	-2.4026294	2.4129E-16
isochorismatase domain containing 2b	Isoc2b	37.1963175	9.264930849	-2.4046983	9.4691E-08
guanylate binding protein 3	Gbp3	203.734903	70.99078971	-2.4111277	1.4109E-12
tripartite motif-containing 34A	Trim34a	63.3314282	15.38785634	-2.4148749	1.4222E-07
lipase, member O2	Lipo2	138.035551	45.84710982	-2.4153821	1.4312E-11
membrane-spanning 4-domains, subfamily A, member 6C	Ms4a6c	21.9909206	0.494068601	-2.4236048	1.945E-08
monoacylglycerol O-acyltransferase 2	Mogat2	382.644819	142.2131286	-2.4717491	3.0321E-23
cDNA sequence BC025446	BC025446	28.744686	3.197460917	-2.5175598	4.2501E-08
V-set immunoregulatory receptor	Vsir	428.620289	158.830207	-2.5191874	3.8613E-29
myomesin 2	Myom2	153.979653	46.06109577	-2.5328666	2.2815E-11
C1q and tumor necrosis factor related protein 3	C1qtnf3	14233.5801	5025.291081	-2.5510381	1.3193E-21
toll-like receptor 13	Tlr13	33.3801578	3.491696513	-2.5645345	2.5013E-08
tumor protein D52-like 1	Tpd52l1	396.10367	141.8797116	-2.5600299	1.0185E-26
neurocalcin delta	Ncald	481.119015	168.480936	-2.5621635	6.8179E-23
activating transcription factor 3	Atf3	479.706989	168.8697578	-2.5732914	2.9985E-26
C-type lectin domain family 5, member a	Clec5a	24.7649355	0.738329341	-2.5785365	1.8876E-09
testis expressed gene 15	Tex15	674.60122	241.1993993	-2.5824382	1.2958E-27
macrophage scavenger receptor 1	Msr1	82.1299824	17.98038831	-2.5841827	6.8423E-09
cell migration inducing protein, hyaluronan binding	Cemip	3938.67541	1386.596372	-2.5977894	3.6703E-26
serine/threonine kinase 26	Stk26	169.936902	53.66883267	-2.6352547	3.9789E-15
ribonuclease T2B	Rnaset2b	64.4920881	14.50798953	-2.6520134	3.4545E-09
aminoadipate-semialdehyde synthase	Aass	142.75778	41.3646705	-2.6613747	2.3247E-13
guanylate binding protein 7	Gbp7	370.466121	123.1087299	-2.6857061	5.7901E-25
regulator of G-protein signaling 4	Rgs4	4211.73911	1468.210273	-2.6950705	5.334E-40
ribosomal protein L34	Rpl34	1239.37663	195.9066733	-2.7009456	4.3832E-09
ribosomal protein L34, pseudogene 1	Rpl34-ps1	1239.37663	195.9066733	-2.7009456	4.3832E-09
predicted gene 4705	Gm4705	1239.37663	195.9066733	-2.7009456	4.3832E-09
C-type lectin domain family 4, member n	Clec4n	24.311901	1.104661858	-2.7187284	1.6862E-09
cell adhesion molecule 1	Cadm1	176.891997	54.17397986	-2.7342009	1.9571E-17
immunity-related GTPase family M member 2	Irgm2	186.244906	52.80559157	-2.7866105	2.6609E-16
poly (ADP-ribose) polymerase family, member 9	Parp9	1074.79941	351.7998527	-2.7900025	4.7634E-34
MX dynamin-like GTPase 2	Mx2	75.8284028	14.63838199	-2.8039933	1.1856E-10
chemokine (C-C motif) ligand 9	Ccl9	157.866027	36.14657386	-2.8120922	1.395E-11
tubulin polymerization promoting protein	Tppp	102.669951	26.95940424	-2.8336009	2.3816E-14
monooxygenase, DBH-like 1	Moxd1	2066.86929	702.783185	-2.864394	4.4897E-97
cytidine monophosphate (UMP-CMP) kinase 2, mitochondrial	Cmpk2	213.873498	61.46241758	-2.8875887	1.0789E-20
TYRO protein tyrosine kinase binding protein	Tyrobp	45.0157997	2.056692005	-2.8913393	1.211E-10
matrix metalloproteinase 12	Mmp12	73.0535392	5.118330533	-3.0086281	3.7734E-11
cytochrome P450, family 4, subfamily a, polypeptide 12B	Cyp4a12b	249.648925	67.34686383	-3.1134707	2.7041E-27
chemokine (C-X3-C motif) receptor 1	Cx3cr1	74.0067207	12.43171464	-3.1206534	5.1736E-13
lymphocyte cytosolic protein 1	Lcp1	110.70374	23.8922186	-3.26211	2.4796E-18
interferon gamma induced GTPase	Igtp	211.828135	44.72298227	-3.264545	6.5627E-18
cytochrome b-245, beta polypeptide	Cybb	58.2279072	5.170961761	-3.2706961	1.0077E-12
XIAP associated factor 1	Xaf1	277.225443	52.98861526	-3.271451	6.0366E-16
adhesion G protein-coupled receptor E1	Adgre1	48.4593625	5.123760465	-3.2875253	6.7451E-13
complement component 1, q subcomponent, beta polypeptide	C1qb	53.7119689	4.998915129	-3.3258967	3.1413E-13
OTU domain containing 7A	Otud7a	398.537016	104.8369304	-3.3393484	1.2395E-40
membrane-spanning 4-domains, subfamily A, member 7	Ms4a7	29.9055157	0.449640866	-3.3779466	4.1648E-14
processing of precursor 4, ribonuclease P/MRP family, (S. cerevisiae)	Pop4	2438.43211	678.2621733	-3.3798818	7.3365E-73
family with sequence similarity 181, member B	Fam181b	140.393082	25.12727291	-3.5182639	9.5681E-18
interferon regulatory factor 7	Irf7	291.734456	66.12520856	-3.6284693	1.0514E-34
guanylate binding protein 2	Gbp2	575.172315	117.2472768	-3.7887929	1.4663E-28
complement component 1, q subcomponent, alpha polypeptide	C1qa	96.0403408	7.260870072	-3.8934177	7.1565E-17
ATPase, H+ transporting, lysosomal V0 subunit C	Atp6v0c	339.649275	64.47130769	-3.9612336	6.6604E-29
macrophage expressed gene 1	Mpeg1	142.382428	20.30606872	-4.0230683	3.1362E-22
complement component 1, q subcomponent, C chain	C1qc	78.6027571	6.639299762	-4.2522126	5.5718E-20
ribosomal protein S18	Rps18	1824.50163	345.4474561	-4.549037	4.5249E-60
ubiquitin specific peptidase 18	Usp18	314.747545	44.34548909	-4.6637025	1.621E-32
spermatogenesis associated glutamate (E)-rich protein 3	Speer3	53.5482083	0	-5.2288727	1.2378E-24
tripartite motif-containing 30A	Trim30a	62.3710788	0.693901606	-5.98552	8.3679E-29
histocompatibility 2, T region locus 23	H2-T23	302.049111	35.03601332	-6.1190391	1.9691E-51
cathepsin S	Ctss	108.592105	6.84178914	-6.3988109	3.8871E-38
lysozyme 2	Lyz2	640.693301	65.33199395	-7.1067361	1.6143E-74
interferon-induced protein 44	Ifi44	454.625564	26.78418172	-8.3869943	4.2967E-53
ribosomal protein S2	Rps2	4790.88714	443.3232484	-9.4032585	6.888E-197
histocompatibility 2, T region locus 22	H2-T22	1002.51961	68.02135051	-12.304463	4.221E-205
histocompatibility 2, T region locus 9	H2-T9	1002.51961	68.02135051	-12.304463	4.221E-205
tripartite motif-containing 30D	Trim30d	149.791915	0	-13.352236	5.0447E-61
tripartite motif-containing 12A	Trim12a	207.539651	0.24426074	-21.544905	8.2444E-89

Table S3: Significantly regulated by the combination of MYC and KRas^{G12D} in MEFs

Table shows RNA-SEQ reads for each gene significantly regulated by more than 2 fold upon combined activation of Rosa26^{DM-lsl-MYC} and lsl-KRas^{G12D} alleles for 24hrs in primary MEFs. Comparison is with identically treated passage-matched wild-type MEFs. FC = fold change, numbers >2 in red; <-2 in dark blue. Adjusted p values <0.05 shown in red.

Table S4: Significantly regulated by MYC or Miz1 depletion in KMC PDAC cells

Mean RNA-SEQ values for expressed genes in KMC cells, with and without siRNA depletion of MYC or Miz1, filtered for genes significantly regulated by MYC depletion. Fold change and Adjusted P values for siMYC and siMiz1, relative to control siRNA-treated KMC cells, shown.

SUPPLEMENTARY METHODS

RNA-SEQ analysis

Pancreatic tumours were removed from euthanised subject animals and dissected into 3-5mm fragments to remove all extraneous (eg. normal, gut or lymph node) tissue. Total RNA was isolated using the RNEasy Mini Kit (Qiagen) according to manufacturer's protocol and DNA was depleted with the RNase-Free DNase Set (Qiagen). Quality of the purified RNA was tested on an Agilent 2200 TapeStation using RNA screentape. For analysis of MEF gene expression, libraries were prepared using the TruSeq stranded totalRNA with RiboZero kit (Illumina). For analysis of bulk tumour gene expression, cDNA libraries were prepared as previously (2), using Illumina TruSeq Stranded mRNA LT Kit. Quality and quantity of the cDNA libraries was assessed on an Agilent 2200 TapeStation (D1000 screentape) and Qubit (Thermo Fisher Scientific) respectively. Libraries were run on an Illumina NextSeq500 using the High Output 75 cycles kit (2x36 cycles, paired end reads, single index). Quality checks on the raw RNA-Seq data files were done using FastQC (3) and Fastq Screen (4). Alignment of the RNA-Seq paired-end reads was to the GRCm38 (5) version of the mouse genome and annotation using HiSat2 (6) and TopHat (7). Expression levels were determined and statistically analysed by a workflow combining HTSeq (8), the R environment (9), utilising packages from the Bioconductor data analysis suite (10) and differential gene expression analysis based on the negative binomial distribution using the DESeq2 package (11). Further data analysis and visualisation used R and Bioconductor packages. Pathway modulation analysis was performed using Metacore GeneGO (12). Gene-set enrichment for PDAC subtype gene signatures was performed on the converted mouse identifiers using the 'GSVA' package (13). PDAC subtype gene signatures are as defined in Bailey et al. (1).

Software Versions for pancreatic tumour analysis:

FastQC version 0.11.7; Fastq Screen version 0.12.0; GRCm38.93 version of the mouse genome and annotation; HiSat2 version 2.1.0; HTSeq version 0.9.1; R environment version 3.4.4

Software Versions for KC pancreatic tumours:

GRCm38.75 version of the mouse genome and annotation; TopHat run version 2.0.13

Software Versions for MEF experiments:

GRCm38.75 version of the mouse genome and annotation; TopHat run version 2.0.13; Bowtie version

2.2.4.0; R environment version 3.3.2

RT-PCR

RNA was isolated using TRIZOL (Invitrogen) method according to manufacturer's directions. Quantitect reverse transcription kit (Qiagen 205313) was used for cDNA synthesis followed by real time PCR using SYBR Green method (VWR QUNT95072). Gusb and ACTIN were used for data normalization in mouse and human samples respectively. The following primer sets were used to detect indicated mRNA transcripts:

Mouse

Gusb F: cacttcgaccacacctagag, R: accgcagggtgattttgt

Irf5 F: tacgaggtctgctccaacg, R: gcctggtagcattctctgga

Irf7 F: cttcagcactttctccgaga, R: tgtagtgggtgacccttgc

Ifi44 F: cacacgtggatagcctggat, R: ggcaaaaccaaagactccat

Ifnb1 F: aactccaccagcagacagt, R: agtggagagcagttgaagac

Myc F: cgcgtccgagtgattga, R: agcagcagtgccaggaa

Miz1 F: tctgtggtggggttcggac, R: ctgctccaagacacgctggc

Cxc13 F: tcacacatataactttctcatcttg, R: catagatcggattcaagttacgc

Human

Actin F: ccaaccgcgagaagatga, R: ccagaggcgtacaggatag

IRF5 F: cacactccagcccacttc, R: gcatctgcacctggaagg

IRF7 F: ctgcagtcacacctgtagcc, R: gtggactgagggtttagc

IFI44 F: agcctgtgaggtccaagcta, R: gcagaaagaattagaacatcctttaca

IFNB1 f: gacgccgattgaccatcta, R: agccaggaggttctcaacaat

Myc F : gccctggtgctccatga, R: caacatcgatttctctcatcttct

SUPPLEMENTARY REFERENCES

1. Bailey P, Chang DK, Nones K, Johns AL, Patch AM, Gingras MC, et al. Genomic analyses identify molecular subtypes of pancreatic cancer. *Nature*. 2016;531(7592):47-52.
2. Fisher S, Barry A, Abreu J, Minie B, Nolan J, Delorey TM, et al. A scalable, fully automated process for construction of sequence-ready human exome targeted capture libraries. *Genome Biol*. 2011;12(1):R1.
3. S. A. FastQC: a quality control tool for high throughput sequence data. 2018.
4. Wingett S. FastQ Screen. 2018.
5. Zerbino DR, Achuthan P, Akanni W, Amode MR, Barrell D, Bhai J, et al. Ensembl 2018. *Nucleic Acids Res*. 2018;46(D1):D754-D61.
6. Kim D, Langmead B, Salzberg SL. HISAT: a fast spliced aligner with low memory requirements. *Nat Methods*. 2015;12(4):357-60.
7. Trapnell C, Pachter L, Salzberg SL. TopHat: discovering splice junctions with RNA-Seq. *Bioinformatics*. 2009;25(9):1105-11.
8. Anders S, Pyl PT, Huber W. HTSeq--a Python framework to work with high-throughput sequencing data. *Bioinformatics*. 2015;31(2):166-9.
9. R Core Team RFFSC, Vienna, Austria. . A language and environment for statistical computing. 2018.
10. Huber W, Carey VJ, Gentleman R, Anders S, Carlson M, Carvalho BS, et al. Orchestrating high-throughput genomic analysis with Bioconductor. *Nat Methods*. 2015;12(2):115-21.
11. Love MI, Huber W, Anders S. Moderated estimation of fold change and dispersion for RNA-seq data with DESeq2. *Genome Biol*. 2014;15(12):550.
12. Analytics C. Metacore.
13. Hanzelmann S, Castelo R, Guinney J. GSEA: gene set variation analysis for microarray and RNA-seq data. *BMC Bioinformatics*. 2013;14:7.